THE JOURNAL OF BIOLOGICAL CHEMISTRY VOL. 288, NO. 5, pp. 3381–3393, February 1, 2013
© 2013 by The American Society for Biochemistry and Molecular Biology, Inc. Published in the U.S.A.

The Non-lysosomal β-Glucosidase GBA2 Is a Non-integral Membrane-associated Protein at the Endoplasmic Reticulum (ER) and Golgi*

Received for publication, August 29, 2012, and in revised form, December 5, 2012 Published, JBC Papers in Press, December 17, 2012, DOI 10.1074/jbc.M112.414714

Heinz G. Körschen[‡1], Yildiz Yildiz[§1], Diana Nancy Raju[‡§], Sophie Schonauer[‡], Wolfgang Bönigk[‡], Vera Jansen[‡], Elisabeth Kremmer[¶], U. Benjamin Kaupp[‡], and Dagmar Wachten[‡2]

From the [‡]Department of Molecular Sensory Systems, Center of Advanced European Studies and Research, Ludwig-Erhard-Allee 2, 53175 Bonn, Germany, [§]Medizinische Klinik I, Universitätsklinikum Bonn, Sigmund-Freud-Strasse 25, 53105 Bonn, Germany, and the [¶]Institute of Molecular Immunology, Helmholtz Zentrum München, Marchioninistrasse 25, 81377 Munich, Germany

Background: The β-glucosidase GBA2 degrades glucosylceramide (GlcCer) outside the lysosomes.
Results: GBA2 is not an integral membrane protein but rather is membrane-associated at the ER and Golgi.
Conclusion: GBA2 is located in a key position for a lysosome-independent route of GlcCer-dependent signaling.
Significance: Understanding the localization and enzymatic properties of GBA2 is crucial for investigating the role of non-lysosomal glucosylceramide in Gaucher disease pathology.

GBA1 and GBA2 are both β-glucosidases, which cleave glucosylceramide (GlcCer) to glucose and ceramide. GlcCer is a main precursor for higher order glycosphingolipids but might also serve as intracellular messenger. Mutations in the lysosomal GBA1 underlie Gaucher disease, the most common lysosomal storage disease in humans. Knocking out the non-lysosomal GBA2 in mice results in accumulation of GlcCer outside the lysosomes in various tissues (*e.g.* testis and liver) and impairs sperm development and liver regeneration. However, the underlying mechanisms are not well understood. To reveal the physiological function of GBA2 and, thereby, of the non-lysosomal GlcCer pool, it is important to characterize the localization of GBA2 and its activity in different tissues. Thus, we generated GBA2-specific antibodies and developed an assay that discriminates between GBA1 and GBA2 without the use of detergent. We show that GBA2 is not, as previously thought, an integral membrane protein but rather a cytosolic protein that tightly associates with cellular membranes. The interaction with the membrane, in particular with phospholipids, is important for its activity. GBA2 is localized at the ER and Golgi, which puts GBA2 in a key position for a lysosome-independent route of GlcCer-dependent signaling. Furthermore, our results suggest that GBA2 might affect the phenotype of Gaucher disease, because GBA2 activity is reduced in *Gba1* knock-out fibroblasts and fibroblasts from a Gaucher patient. Our results provide the basis to understand the mechanism for GBA2 function *in vivo* and might help to unravel the role of GBA2 during pathogenesis of Gaucher disease.

Glycosphingolipids (GSLs)[3] in cell membranes from bacteria to humans fulfill a variety of functions (*e.g.* promoting cell growth and differentiation, mediating cell-cell adhesion, and serving as signaling receptors) (1). The mode of action depends on the concentration and distribution of GSLs in the membrane. Up to 400 different GSLs have been identified that vary in their sugar chain structure (2). One of the main precursors for GSLs is glucosylceramide (GlcCer). GlcCer is synthesized by glucosylation of ceramide via a glucosylceramide synthase at the cytosolic side of the Golgi complex (3–5). Higher order GSLs are formed by adding monosaccharides to the glucosyl headgroup in the Golgi lumen (6, 7). These modifications require GlcCer transport from the cytosolic to the lumenal side of the Golgi. Two models of GlcCer transport have been proposed. One model suggests that GlcCer reaches the lumenal side at the endoplasmic reticulum (ER) rather than at the Golgi (8, 9). According to this model, GlcCer is first transported to the ER by FAPP2 (phosphatidylinositol 4-phosphate adaptor protein) and then flipped to the lumenal side by low specificity phospholipid flippases (8, 9). From the ER, GlcCer reaches the Golgi lumenal side by vesicular transport. Another model also involves FAPP2, but here FAPP2 transports GlcCer from the *cis*-Golgi network to the *trans*-Golgi network, where a yet unidentified transporter flips GlcCer to the lumenal side (10). Apart from these two pathways, a fraction of GlcCer is also transported to the plasma membrane via non-vesicular transport, where it is inserted into the cytosolic membrane leaflet (9). Transport of GlcCer to the plasma membrane has been proposed to involve FAPP2 and another glucosylceramide transfer protein, GLTP (glycolipid transfer protein) (9).

GlcCer is degraded to glucose and ceramide by three different hydrolases: the lysosomal GBA1 and the non-lysosomal GBA2 and GBA3 (11–16). The three GBA proteins show no structural or sequence homology but share a similar enzymatic

* This work was supported by Deutsche Forschungsgemeinschaft Grant SFB 645.
[1] Both authors contributed equally to this work.
[2] To whom correspondence should be addressed. Tel.: 49-228-9656-311; Fax: 49-228-9656-9311; E-mail: dagmar.wachten@caesar.de.
[3] The abbreviations used are: GSL, glycosphingolipid; GlcCer, glucosylceramide; GBA, β-glucosidase; FPP, fluorescence protease protection; PNS, postnuclear supernatant; PC, phosphatidylcholine; rfu, relative fluorescence units; ICC, immunocytochemistry; WB, Western blot; eGFP, enhanced green fluorescent protein; aa, amino acids; MU, methylumbelliferyl; NB-DNJ, *N*-butyldeoxynojirimycin; PrP, prion protein; CBE, conduritol B epoxide.

activity. Degradation of GlcCer has been mainly studied for the lysosomal route; GlcCer reaches the lysosomes through the endosomal pathway and is degraded in the lysosome lumen by GBA1. Mutations in the *Gba1* gene cause Gaucher disease, a severe lysosomal storage disorder characterized by accumulation of GlcCer in tissue macrophages (17, 18). Although the activity of a non-lysosomal β-glucosidase was described as early as 1993 (13), the mechanism and function of non-lysosomal GlcCer degradation is not well understood. GBA3 is a cytosolic, Klotho-related protein; members of this family share a β-glucosidase-like domain (11, 12, 14), but their physiological function is not known.

The other non-lysosomal β-glucosidase GBA2 (15, 19) has been proposed to be a single-pass transmembrane protein with a long N terminus containing the β-glucosidase domain followed by one transmembrane domain and a shorter C terminus (20). Further studies suggest that (*a*) the C-terminal part is cytosolic and the N-terminal part is located either in the lumen of an organelle or on the extracellular side, and (*b*) GBA2 is located at or close to the cell surface (19). GBA2 mRNA is rather ubiquitously expressed with higher levels in testis, brain, and liver (15). GBA2-deficient mice accumulate GlcCer in particular in those tissues that express GBA2 most prominently. Accumulation of GlcCer has mainly two consequences: (*a*) male fertility is impaired due to the formation of aberrant sperm, and (*b*) liver regeneration after partial hepatectomy is delayed (15, 21). The mechanisms underlying these phenotypes are ill defined, because the signaling function of GlcCer is not well understood. In particular, the fate of non-lysosomal GlcCer (*i.e.* the dynamics and sites of synthesis and breakdown) is unknown.

Here, we have investigated the topology and localization of GBA2 in heterologous and native systems and analyzed β-glucosidase activity in different tissues. Our results require major revision of existing concepts regarding the topology and localization of GBA2 but also regarding the monitoring of GBA2 activity in particular and β-glucosidase activity in general.

EXPERIMENTAL PROCEDURES

Cloning—The open reading frame of mouse GBA2 (NM_172692) was amplified from cDNA using specific primers containing restriction sites and a Kozak sequence in front of the start codon. The sequence encoding a hemagglutinin (HA) tag was added by PCR either at the 5′- or 3′-end. PCR products were subcloned into pcDNA3.1+ (Invitrogen) and their sequence was verified. The resulting constructs were designated pc3.1-mGBA2-HA (GBA2-HA) and pc3.1-HA-mGBA2 (HA-GBA2). To generate GBA2-eGFP fusion constructs, the open reading frame of mouse GBA2 was subcloned into pEGFP-N1 or pEGFP-C1 (Clontech), generating pEGFP-N1-GBA2 (eGFP-GBA2) and pEGFP-C1-mGBA2 (GBA2-eGFP), respectively.

Antibody Generation—Peptides comprising amino acids (aa) 37–51 (peptide 1), aa 358–377 (peptide 2), aa 505–529 (peptide 3), and aa 720–744 (peptide 4) from the murine GBA2 protein were synthesized and coupled to BSA and ovalbumin (PSL, Heidelberg). Rats were immunized subcutaneously and intraperitoneally with a mixture of 50 μg of peptide-ovalbumin, 5 nmol of CPG oligonucleotide (Tib Molbiol), 500 μl of PBS, and 500 μl of incomplete Freund's adjuvant. A boost without adjuvant was given 6 weeks after the primary injection. Fusion was performed using standard procedures. Supernatants were tested in a differential ELISA with the respective GBA2 peptide and non-related peptides coupled to BSA. Monoclonal antibodies that reacted specifically with GBA2 were further analyzed by Western blot (WB). Tissue culture supernatant of the 4A12 rat IgG1 subclass was used for ICC, and supernatants of 2H1 rat IgG2a, 2F8 rat IgG2b, and 5A8 rat IgG2a were used for WB (see Fig. 1*A*).

Generation of Stable Cell Lines—HEK293 cells were electroporated with pc3.1-mGBA2-HA or pc3.1-HA-mGBA2 using the Neon 100 μl kit (Invitrogen) and the MicroPorator (Digital Bio) according to the manufacturer's protocol (3 × 1245 mV pulses with 10 ms pulse width). Cells were transferred into complete medium composed of DMEM plus GlutaMax (Invitrogen) and 10% fetal bovine serum (Biochrom). For the selection of monoclonal HEK293 cells stably expressing GBA2, the antibiotic G418 (800 μg/ml; Invitrogen) was added 24 h after electroporation. Monoclonal cell lines were identified by WB and immunocytochemistry using GBA2-specific antibodies.

Fibroblasts—Embryonic fibroblasts from *Gba1* knock-out mice were kindly provided by Ellen Sidransky (National Institutes of Health) (22). Human control fibroblasts were a kind gift from Klaus Harzer (Tübingen University). Fibroblasts from a Gaucher patient were kindly provided by Mia Horowitz (Tel Aviv University). The patient displayed Gaucher disease type II with a L444P/P415R genotype. Fibroblasts are grown in complete medium composed of DMEM, 2 mM L-glutamine, 1 mM sodium pyruvate, penicillin/streptomycin (all from Invitrogen), and 10% FCS (Biochrom) at 37 °C and 5% CO_2 in a humidified incubator.

Primary Hippocampal Neurons—Hippocampal neurons were prepared from embryonic mice at embryonic day 17. Total brains were removed and placed in ice-cold Hanks' balanced salt solution (Invitrogen). Hippocampi were dissected and incubated in trypsin/EDTA for 8 min at 37 °C. The reaction was stopped by adding 10 ml of plating medium (DMEM supplemented with 10% horse serum, penicillin/streptomycin, L-glutamine, 1 mM sodium pyruvate). Hippocampi were washed and resuspended in Hanks' balanced salt solution by gently pipetting up and down. The suspension was diluted in plating medium, and 80,000 cells were seeded on 13-mm glass coverslips coated with poly-D-lysine (Sigma catalog no. P7886). Cells were grown in a humidified incubator at 37 °C with 5% CO_2. After 24 h, plating medium was exchanged for Neurobasal medium (supplemented with 1× B27 serum-free supplement, penicillin/streptomycin, and GlutaMax). After 3 days in culture, 2 μM arabinosylcytosine (Sigma catalog no. C1768) was added to the wells to inhibit growth of glial cells. Media and chemicals were purchased from Invitrogen if not noted otherwise.

GBA2-deficient Mice—The generation of GBA2-deficient mice has been described elsewhere (15). All experiments involving animals were in accordance with the relevant guidelines and regulations.

Immunocytochemistry—Cells on glass coverslips were fixed for 10 min with 4% paraformaldehyde in PBS. To block nonspecific binding sites, cells were incubated for 30 min with blocking buffer (0.5% Triton X-100 and 5% chemiblocker (Millipore, Germany) in 0.1 M phosphate buffer, pH 7.4). Primary antibodies were diluted in blocking buffer and incubated for 1 h at room temperature. After washing with PBS, cells were incubated with fluorescent secondary antibodies diluted in blocking buffer containing 0.5 μg/μl DAPI (Invitrogen). After washing with PBS, cells were mounted on slides and examined with a confocal microscope (Olympus FV1000).

Antibodies—Primary antibodies were as follows: 4A12 (for WB, 1:50, for ICC, 1:20), 2H1, 2F8, 5A8 (for WB, 1:20), calnexin (Sigma catalog no. C4731, for WB, 1:20,000; Abcam catalog no. ab31290, for ICC, 1:100), GM-130 (BD Transduction Laboratories catalog no. 610822, for WB, 1:1000, for ICC, 1:100), giantin (Abcam catalog no. ab24586, for ICC, 1:1,000), β-tubulin-CY3 (Sigma catalog no. C4585, for ICC, 1:200), GFAP (DAKO catalog no. Z0334, for ICC, 1:500), HA (Roche Applied Science catalog no. 11867431001, for ICC 1:1,000, for WB, 1:10,000). Secondary antibodies were as follows: for WB, IRDye680 and IR800 antibodies (LI-COR, 1:20,000); for ICC, fluorescently labeled antibodies (Dianova, 1:500).

Fluorescence Protease Protection Assay—The fluorescence protease protection (FPP) assay has been performed as described elsewhere (23). Images were taken with a ×60 objective using the Olympus CellR microscope.

Nocodazole Treatment—To depolymerize microtubules, cells were incubated in DMEM complete medium containing 2.5 μg/ml nocodazole (Sigma). Cells were incubated at 37 °C and 5% CO_2 for 2.5 h. For repolymerization, cells were washed with medium and incubated for 10 min at 37 °C and 5% CO_2.

Preparation of Cell and Tissue Lysates—All steps are performed at 4 °C in the presence of mammalian protease inhibitor mixture (Sigma-Aldrich). Tissues or HEK293 cells were homogenized in hypotonic buffer (10 mM HEPES/NaOH, 0.5 mM EDTA, pH 7.4; 10 ml/g wet weight of the organ or cell pellet) by using an Ultra-Turrax homogenizer (IKA, Staufen, Germany) and three pulses (20 s each) of sonification (Branson sonifier, Schwäbisch Gmünd, Germany). The suspension (total lysate) was centrifuged for 20 min at 1,000 × *g*. The supernatant (post-nuclear supernatant (PNS)) was used for either activity assays or WB analysis.

Analysis of Membrane Association—PNS was washed three times with hypotonic buffer (10 mM HEPES/NaOH, 0.5 mM EDTA, pH 7.4) and two times with carbonate buffer (100 mM, pH 11.5) After each washing step, the suspension was centrifuged for 20 min at 541,000 × g_{av} (TLA 100.3, Beckman). The membrane pellets obtained after each washing step were designated P1–P5, and the corresponding supernatants were named S1–S5. For Western blot analysis and activity assays, comparable amounts of each fraction were used.

Reconstitution Experiments—Supernatants were prepared from hypotonic lysates (4 mg/ml protein) of brain from wild-type mice or from HEK293 cells overexpressing GBA2. P3 membrane pellets devoid of GBA2 were prepared from hypotonic lysates (4 mg/ml protein) of brain from GBA2-deficient mice or from HEK293 control cells. Furthermore, membranes were isolated from lysates (4 mg/ml protein) of bovine rod outer segments as described elsewhere (24). Preparation of artificial, protein-free membranes composed of soybean L-α-phosphatidylcholine (PC liposomes) has also been described elsewhere (25). Briefly, 50 mg of PC were solubilized in 5 ml of hypotonic buffer containing 36 mM CHAPS and 5 mM DTT. CHAPS was removed by dialysis for 12 h against an 800-fold volume excess of hypotonic buffer. Dialysis was repeated two times. S1 supernatants were mixed with either P3 pellets or bovine rod outer segment membranes. The final concentration of PC for reconstitution experiments was 1 mg/ml. Before performing the activity assay, the mixture of supernatants and membranes was incubated for 30 min at room temperature.

Western Blot Analysis—All samples were heated for 5 min at 95 °C prior to separation on SDS-PAGE. For WB analysis, proteins were transferred onto PVDF membranes, probed with antibodies, and analyzed using the Odyssey Imaging System (LI-COR).

Fluorescence-based GBA Activity Assays—The activity of cellular GBAs was analyzed using 4-methylumbelliferyl-β-D-glucopyranoside (4-MU-β-D-glucopyranoside) (Sigma) (26, 27) as a fluorescent substrate. Cleavage of 4-MU-β-D-glucopyranoside was monitored in real time in a Fluostar Omega reader (BMG Labtech) at 29 °C using the filter pair 355 nm/460 nm for excitation and emission, respectively. The assays were performed in 384-well plates (Greiner) in the plate mode. Per well, 25 μl of lysate containing 5–10 μg of total protein were provided. To discriminate between GBA1 and GBA2 activity, conduritol B epoxide (CBE) (Sigma), an inhibitor for GBA1, or *N*-butyldeoxynojirimycin (NB-DNJ) (Sigma-Aldrich), an inhibitor for GBA2, were included. The pH of protein lysates and the 4-MU-β-D-glucopyranoside solution was adjusted by diluting with McIlvaine buffer. The assay was initiated by adding 5 μl of 4-MU-β-D-glucopyranoside (10 mM), resulting in a final substrate concentration of 1.67 mM. The hydrolysis of 4-MU-β-D-glucopyranoside was recorded as a change in relative fluorescence units (rfu)/min. Each analysis was performed as a quadruplicate in parallel. Per genotype, tissues or cells from three animals were analyzed if not otherwise stated. Data analysis was performed using Origin software (OriginLab).

RESULTS

Generation of GBA2-specific Antibodies—An in depth characterization of GBA2 localization had been hampered so far by the lack of suitable antibodies. Therefore, we generated monoclonal antibodies against four different epitopes located in different regions of the GBA2 protein (Fig. 1*A*). We tested the specificity of the antibodies by Western blot and immunocytochemistry using testes from GBA2 wild-type and knock-out mice and from HEK293 cells expressing GBA2 fused to an HA tag. All GBA2 antibodies specifically detected the overexpressed protein in HEK293 lysates and the native protein in wild-type testis lysates; no protein was detected in lysates from HEK293 control cells or knock-out testis (Fig. 1*B*). The GBA2-specific antibody (4A12) and the HA antibody produced similar staining patterns in HEK293 cells overexpressing GBA2-HA (Fig. 1*C*). Thus, these antibodies represent specific and sensitive tools for further studies.

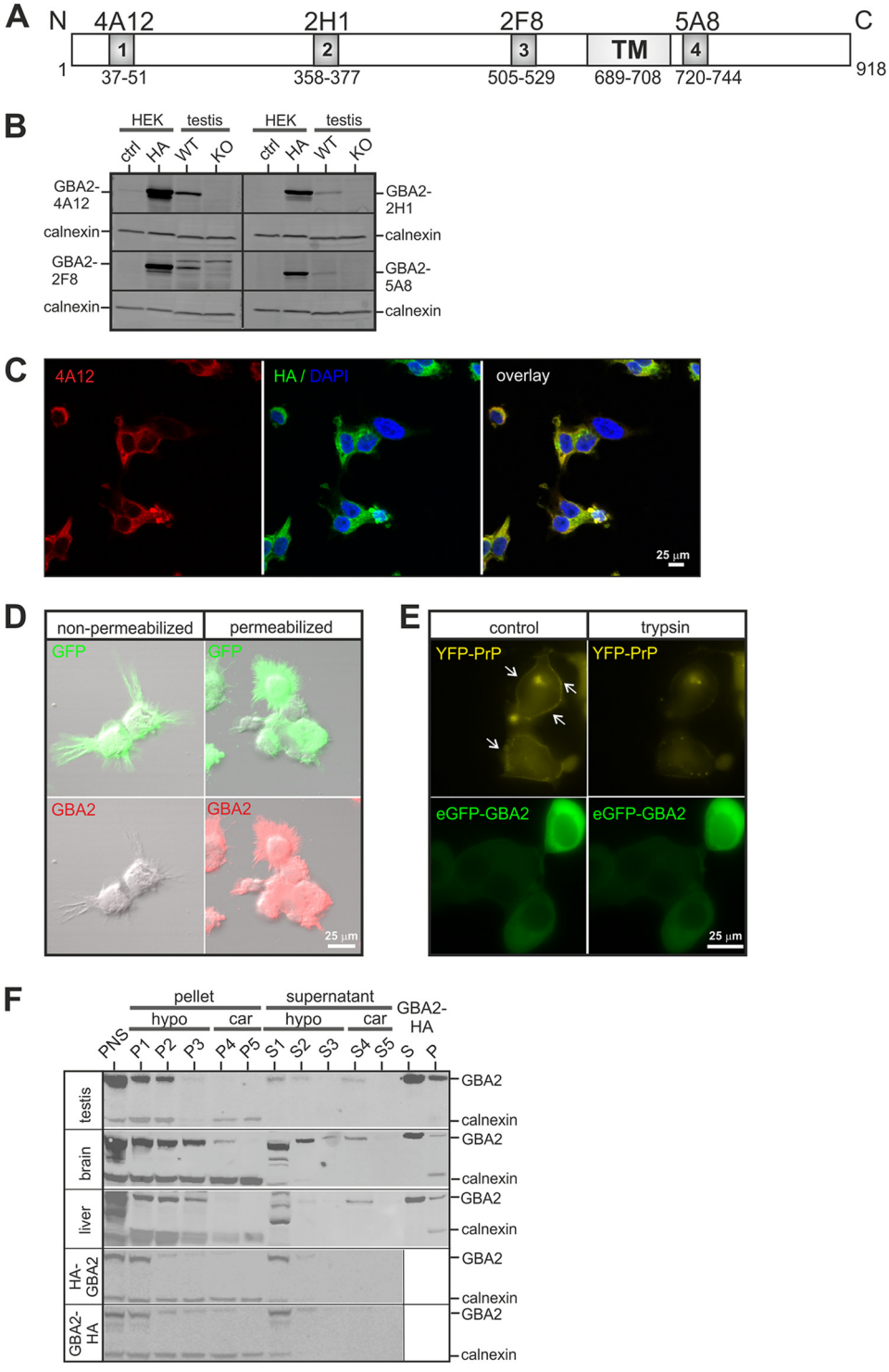

FIGURE 1. **GBA2 is a non-integral membrane-associated protein.** *A*, topology of mouse GBA2. Amino acid positions, the putative transmembrane domain (*TM*), and epitopes for the GBA2-specific antibodies (4A12, 2H1, 2F8, and 5A8; *gray boxes*, *1–4*) are indicated. *B*, to validate GBA2-specific antibodies, Western blots of total lysates from HEK293 wild-type cells (*ctrl*), from HEK293 cells overexpressing GBA2-HA (*HA*), and from wild-type (*WT*) and *Gba2* knock-out (*KO*) testis were performed using different anti-GBA2 antibodies. Calnexin was used as a loading control. *C*, HEK293 cells overexpressing GBA2-HA were labeled with the 4A12 (*red*) and HA antibody (*green*), followed by the corresponding fluorescently labeled secondary antibody. DAPI (*blue*) has been used to label DNA. *Scale bar*, 25 μm. *D*, non-permeabilized and Triton X-100-permeabilized HEK293 cells overexpressing GBA2 were labeled with the 4A12 antibody (*red*), followed by the corresponding fluorescently labeled secondary antibody. GFP (*green*) was used as a control. *Scale bar*, 25 μm. *E*, HEK293 cells were transfected with YFP-PrP (positive control; fusion between the GPI-anchored PrP and YFP; *yellow*) or eGFP-GBA2 (*green*). Cells were treated with trypsin for 1 min and imaged before (*control*) and after trypsin incubation (*trypsin*). *Arrows* highlight fluorescence of YFP-Prp at the plasma membrane. *Scale bar*, 25 μm. *F*, hypotonic lysates from liver, brain, testis, and HEK293 cells overexpressing GBA2-HA or HA-GBA2 were centrifuged at low speed. The supernatant (PNS) was subjected to high speed centrifugation, and the resulting pellet was subjected to multiple hypotonic (*hypo*) and carbonate washes (*car*). The corresponding pellet fractions (*P*) and supernatants (*S*) have been subjected to Western blotting and labeled with anti-GBA2 antibodies (mixture of 4A12/2F8). Calnexin was used as a loading control.

GBA2 Is a Non-integral Membrane-associated Protein—It has been reported that GBA2 behaves like an integral membrane protein with its N terminus, containing the catalytic domain, being accessible to substrates in the extracellular space (19). However, GlcCer is located in the inner leaflet of the plasma membrane, making it difficult to explain how GBA2 reaches the substrate. To solve this conundrum, we tested whether the N terminus of GBA2 is extracellularly located using a monoclonal antibody (4A12) raised against an N-terminal epitope (Fig. 1*A*). In HEK293 cells overexpressing GBA2, the antibody detected the protein only in Triton X-100-permeabilized cells (Fig. 1*D*). We corroborated this result using an FPP assay (23) that allows for determination of the topology and localization of fluorescent fusion proteins in living cells (Fig. 1*E*). The FPP assay provides a fluorescent readout before and after protein degradation by trypsin. Under non-permeabilizing conditions, treatment with trypsin readily degrades protein moieties facing the extracellular side but spares those facing the cytosolic side. To investigate whether the N terminus of GBA2 is facing the extracellular side, cells were imaged before and after trypsin treatment (4 mM, 1 min). As a control, HEK293 cells were transfected with YFP-PrP, a fusion between the GPI-anchored prion protein (PrP) and the yellow fluorescent protein (YFP). In the control, the distinctive fluorescence at the cell surface disappeared after trypsin treatment (Fig. 1*E*). In contrast, cells expressing GBA2 with a green fluorescent protein (eGFP) attached to its N terminus showed no change in fluorescence after trypsin treatment (Fig. 1*E*), indicating that the N terminus is not accessible from the extracellular side.

To test whether GBA2 is an integral membrane protein at all, we used a biochemical approach. Cells or tissues were lysed in hypotonic buffer, and proteins were separated into soluble and membrane fractions and tested for the presence of GBA2 by immunoblotting. GBA2 was detected in both membrane and soluble fractions (Fig. 1*F*). Hypotonic washes resulted in the loss of GBA2 from the membrane fraction and recovery in the soluble fraction (Fig. 1*F*). In HEK293 cells overexpressing GBA2, the protein was almost completely recovered in the soluble fraction after the first hypotonic wash, whereas in native tissue from brain, testis, and liver, hypotonic washes did not fully remove GBA2 from the membrane fraction. However, after a carbonate wash, which allows quantitative distinction between peripheral and integral membrane proteins (28), GBA2 was fully recovered in the supernatant (Fig. 1*F*). These results demonstrate that GBA2 is not an integral membrane protein but rather is tightly associated with membranes.

GBA2 Is Localized at the ER and Golgi—To reveal where GBA2 is localized in a cell, we analyzed GBA2 expression in HEK293 cells using different organelle markers. GBA2 was expressed in the cytosol, but its expression also spatially overlapped with calnexin, an ER marker; with GM130, a marker for the *cis*-Golgi network; and with giantin, a marker for the Golgi cisternae (Fig. 2*A*). When treating cells with nocodazole to depolymerize microtubules and disperse the Golgi, the GBA2 expression pattern changed (Fig. 2*B*), indicating that GBA2 localization depends on microtubule dynamics. After Golgi dispersal, overlap of GBA2 and giantin expression persisted, at least partially, demonstrating that GBA2 co-segregates with Golgi compartments (Fig. 2*B*). Upon repolymerization (*i.e.* when the Golgi complex formed again), GBA2 still co-segregated with Golgi compartments (Fig. 2*B*). Thus, GBA2 is localized at membranes of both the Golgi and the ER (*i.e.* structures that both rely on microtubule dynamics).

To investigate whether GBA2 is facing the lumenal or the cytosolic side of the ER, we performed an FPP assay under permeabilizing conditions using fluorescently tagged GBA2 constructs (Fig. 2*C*). We used CD3δ-CFP and YFP-CD3δ as controls with the fluophore facing the cytosolic or lumenal side of the ER, respectively (23) (Fig. 2*C*). Images were taken before and after permeabilization with digitonin (20 μM, 1 min) and treatment with trypsin (4 mM, 1 min). The fluorescence of CD3δ-CFP readily changed after incubation with digitonin and trypsin, whereas the fluorescence of YFP-CD3δ did not change, indicating that only protein moieties facing the cytosolic side were degraded (Fig. 2*C*). Under those conditions, the fluorescence of eGFP, which was either fused to the N or the C terminus of GBA2, was readily diminished, indicating that both termini are facing the cytosolic side (Fig. 2*C*).

The expression pattern of GBA2, overexpressed in HEK293 cells, and of the native protein might be different. Therefore, we performed co-localization studies using primary cells. The highest expression levels of GBA2 are observed in testis and brain (15). In brain, GBA2 is expressed in all areas we tested: midbrain, olfactory bulb, cerebellum, hippocampus, and cortex (Fig. 3*A*). We isolated hippocampal neurons from embryonic mice and differentiated the cells in a co-culture with astrocytes. GBA2 was expressed in neurons but not in astrocytes (Fig. 3*B*). The GBA2 expression pattern overlapped with the ER marker calnexin and the *cis*-Golgi marker GM-130 but not with giantin (Fig. 3*C*). These results show that the endogenous GBA2 expression pattern in neurons and in heterologous systems is similar; GBA2 is localized at ER and Golgi membranes with the N and C terminus facing the cytoplasm (for an overview, see Fig. 3*D*).

Differential Assay for GBA1 and GBA2 Activity—To reveal the mechanism of non-lysosomal GlcCer breakdown, it is important to precisely distinguish between non-lysosomal GBA2 and lysosomal GBA1 activity. Standard assays used for more than 40 years contain detergents to probe the lysosomal GBA1 activity (29, 30). Although GBA2 is highly expressed in murine liver (15), β-glucosidase activity in liver lysates toward 4-MU-β-D-glucopyranoside under detergent-containing conditions (0.25% Triton X-100, 0.25% sodium taurocholate, 4 mM β-mercaptoethanol, 0.5 mM EDTA) seemed to be solely due to GBA1 (Fig. 4*A*). We measured pH profiles of β-glucosidase activity in liver lysates in the absence or presence of CBE, a blocker for GBA1 activity (31), and NB-DNJ, a blocker for GBA2 activity (32). Whereas CBE reduced β-glucosidase activity, NB-DNJ had no pronounced effect (Fig. 4*A*), suggesting that liver lysates contain GBA1 but no GBA2 activity. We were puzzled by this result and, therefore, scrutinized the assay under detergent-containing conditions using lysates from HEK293 cells overexpressing GBA2 (Fig. 4*B*). β-Glucosidase activity in those cells was partially blocked by CBE or NB-DNJ (Fig. 4*B*), indicating that both GBA1 and GBA2 activity contribute to the total β-glucosidase activity. In the presence of both blockers, a

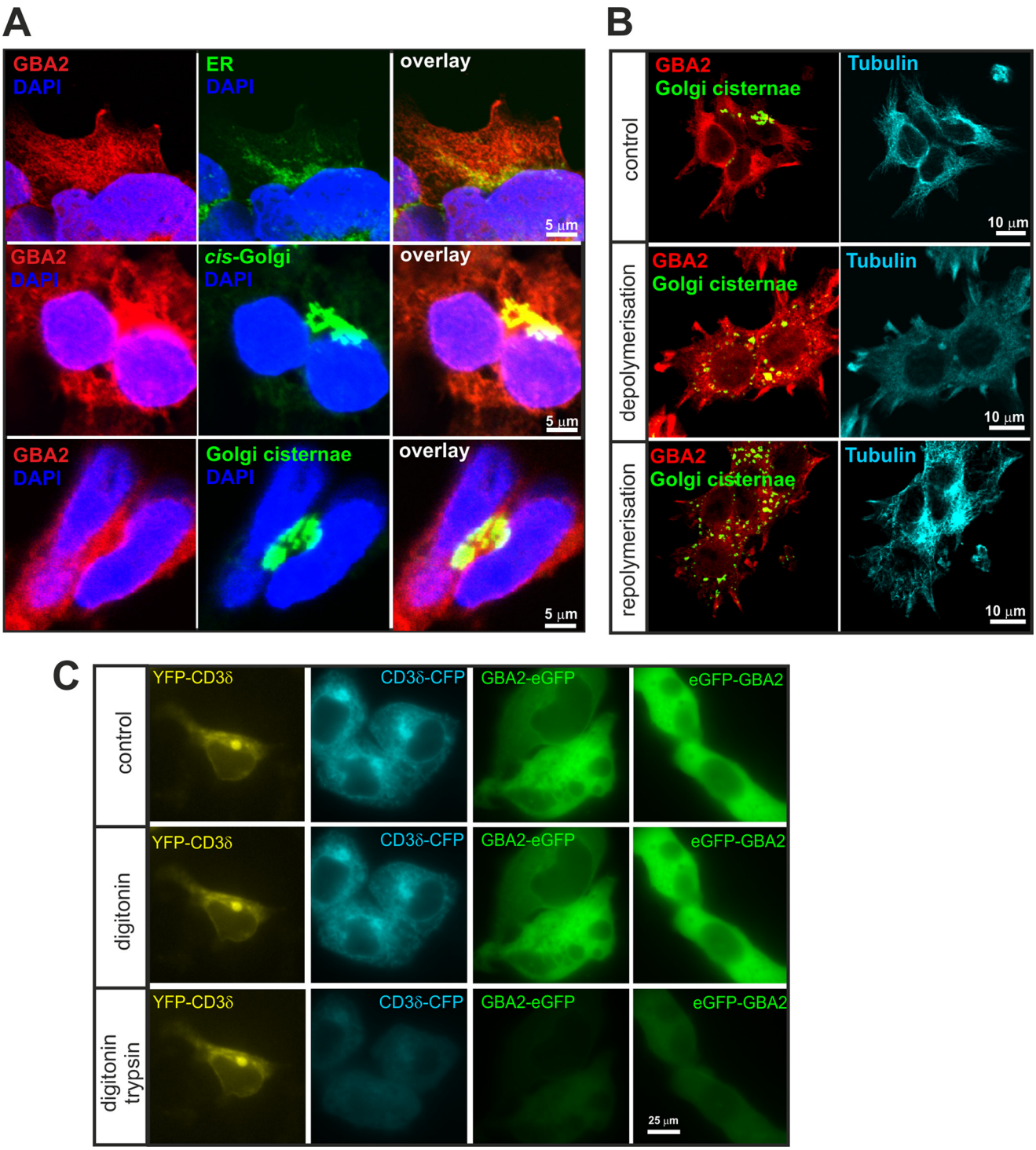

FIGURE 2. **GBA2 is localized at the ER and Golgi in HEK293 cells.** *A*, to analyze the subcellular localization, HEK293 cells overexpressing GBA2 were labeled with the following antibodies: 4A12 (*GBA2*; *red*), calnexin (*ER*; *green*), GM-130 (*cis-Golgi*; *green*), and giantin (*Golgi cisternae*; *green*) followed by the corresponding fluorescently labeled secondary antibody. DAPI (*blue*) was used to label DNA. *Scale bar*, 5 μm. *B*, to depolymerize microtubules, HEK293 cells overexpressing GBA2 were treated with 2.5 μg/ml nocodazole for 2.5 h. After wash-out of nocodazole, microtubules repolymerized again. Antibodies were those described in *A* and β-tubulin-CY3 (*cyan*). *Scale bar*, 10 μm. *C*, to reveal the topology of GBA2, HEK293 cells have been transfected with GBA2-eGFP or eGFP-GBA2 (*green*). YFP-CD3δ (YFP facing the ER lumen; *yellow*) and CD3δ-CFP (CFP facing the cytosolic side; *cyan*) have been used as a control. Cells were imaged before (*control*), after treatment with 20 μM digitonin, and after treatment with 4 mM trypsin for 1 min each. *Scale bar*, 25 μm.

residual activity between pH 4.5 and 7.5 was observed. These results show that both GBA1 and GBA2 activity can be measured under detergent-containing conditions. However, at pH 5.5–6.0, where GBA1 activity has been determined in the past (30, 33), GBA1 and GBA2 activity overlap (Fig. 4*B*). Thus, detergent-containing assay conditions do not allow to clearly distinguish between GBA1 and GBA2 activity, even in the presence of blockers.

To overcome this shortcoming, we tested various assay conditions to rigorously distinguish between lysosomal GBA1 and

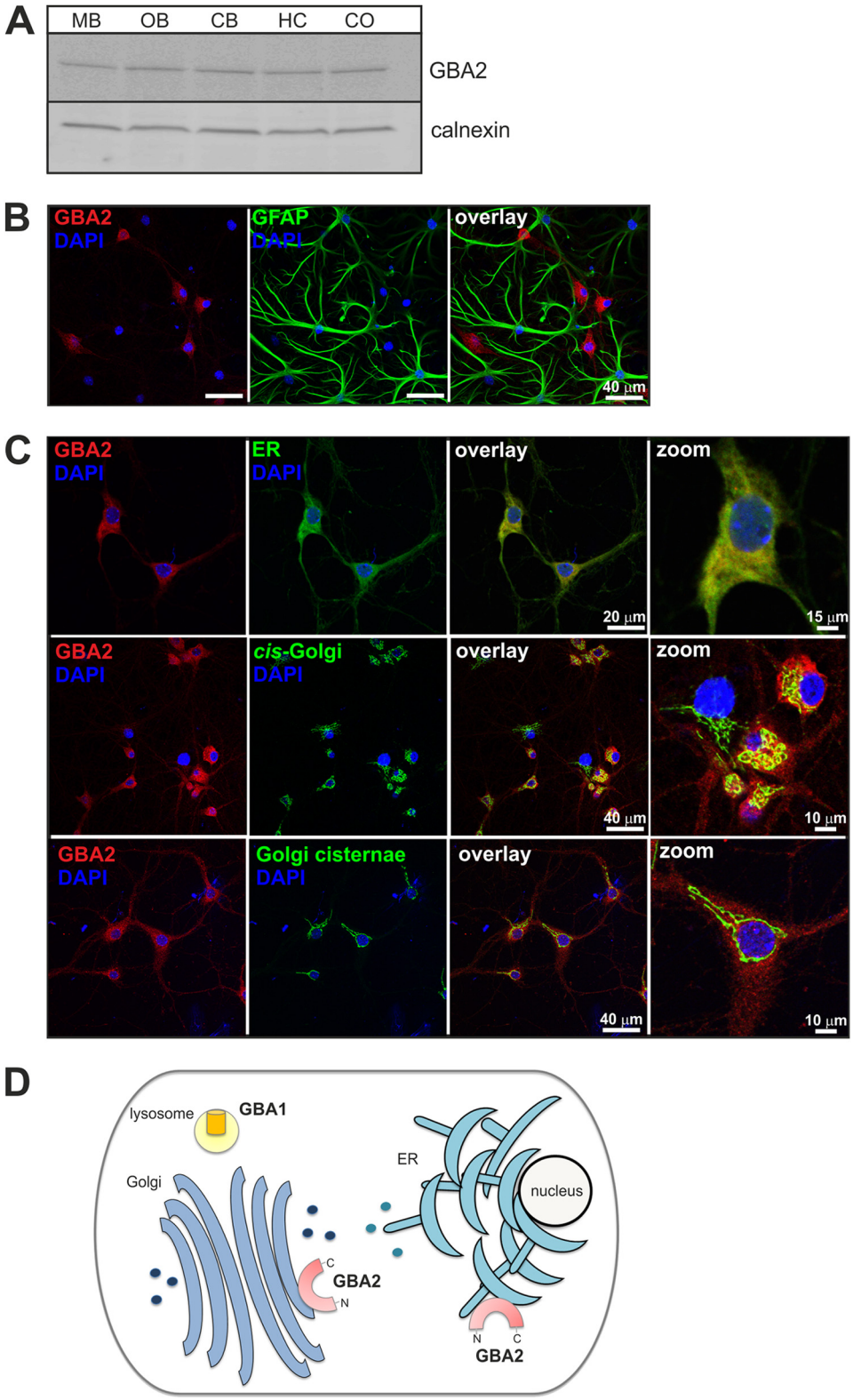

FIGURE 3. **GBA2 is localized at the ER and Golgi in hippocampal neurons.** *A*, to analyze the expression of GBA2 in mouse brain, Western blots of total lysates from different brain regions (*MB*, midbrain; *OB*, olfactory bulb; *CB*, cerebellum; *HC*, hippocampus; *CO*, cortex) were labeled with a GBA2 antibody. Calnexin was used as a loading control. *B*, to analyze the localization of GBA2 in the hippocampus, hippocampal neurons were isolated from mouse embryos at embryonic day 17 and co-cultured with astrocytes. Cells were labeled with a GBA2 antibody (4A12; *red*) and a GFAP-antibody (astrocyte marker; *green*) followed by the corresponding fluorescently labeled secondary antibody. DAPI (*blue*) was used to label DNA. *Scale bar*, 40 μm. *C*, to analyze the subcellular localization of GBA2 in hippocampal neurons, cells were labeled with the following antibodies: 4A12 (*GBA2*; *red*), calnexin (*ER*; *green*), GM-130 (*cis-Golgi*; *green*), and giantin (*Golgi cisternae*; *green*), followed by the corresponding fluorescently labeled secondary antibody. *Scale bars* are indicated. *D*, schematic representing the topology and intracellular localization of GBA2.

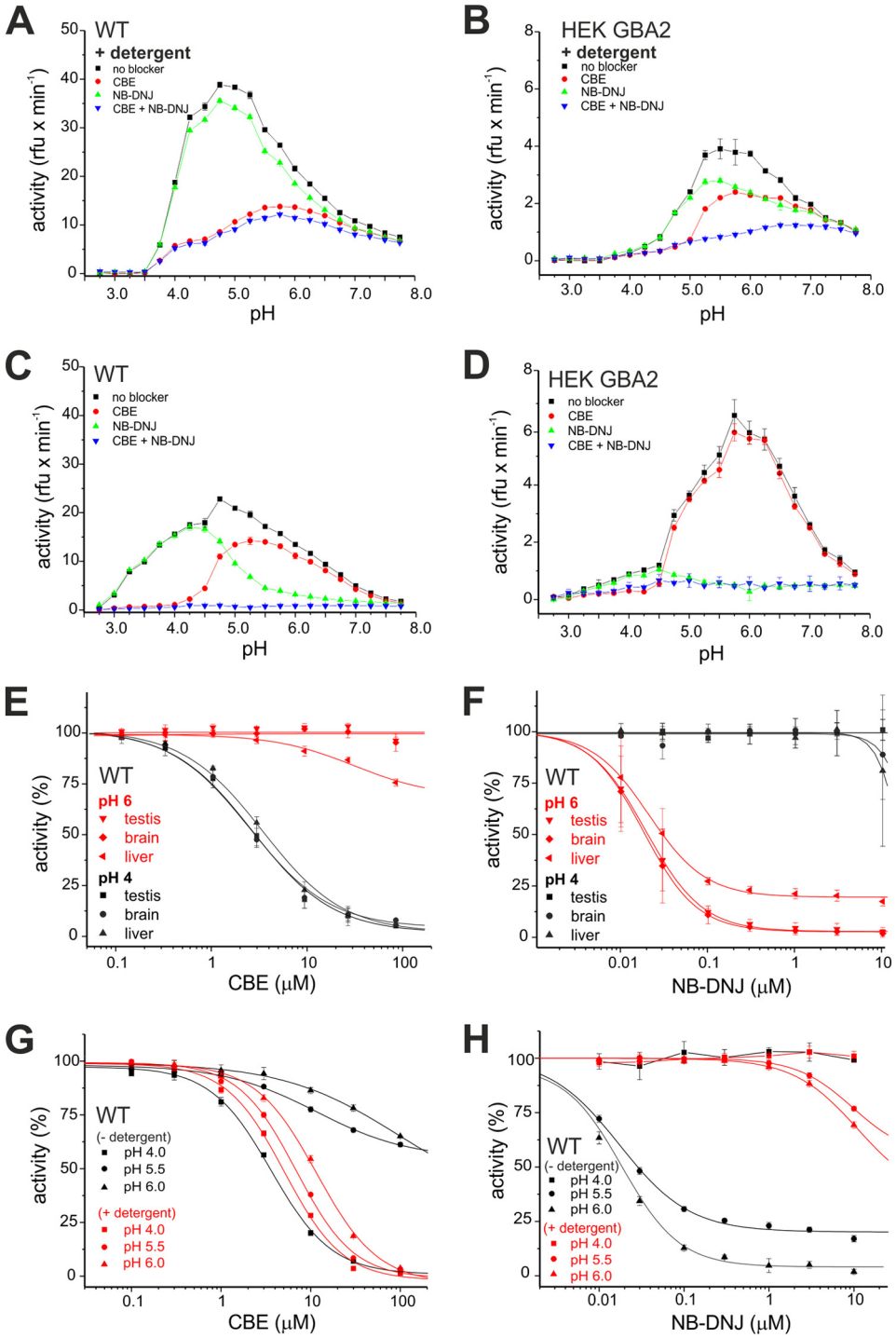

FIGURE 4. **Fluorescence-based β-glucosidase activity assay distinguishes between GBA1 and GBA2 activity in HEK293 cells and native tissue.** *A*, pH dependence of β-glucosidase activity in the presence of detergent in liver from wild-type mice. Activity was measured in lysates containing 0.25% Triton X-100, 0.25% sodium taurocholate, and 4 mM β-mercaptoethanol using a 1.67 mM concentration of the artificial substrate 4-MU-β-D-glucopyranoside in the absence (no blocker) or presence of 30 μM CBE, 10 μM NB-DNJ, or both. *B*, as in *A* for HEK293 cells overexpressing GBA2. *C*, pH dependence of β-glucosidase activity in the absence of detergent in liver of wild-type (*WT*) mice. Activity was measured in hypotonic lysates using a 1.67 mM concentration of the artificial substrate 4-MU-β-D-glucopyranoside in the absence (no blocker) or presence of 30 μM CBE, 10 μM NB-DNJ, or both. *D*, as in *C* for HEK293 cells overexpressing GBA2. All data are presented as mean ± S.D. (*error bars*) ($n = 3$). *E*, dose-response relationship for CBE at pH 4 and 6 in the absence of detergent in liver, brain, and testis of wild-type mice. Maximal activity was set to 100%. IC_{50} values at pH 4 were as follows: liver, 3.5 ± 0.4 μM; brain, 2.5 ± 0.3 μM; testis, 2.7 ± 0.3 μM. *F*, as in *E* for NB-DNJ. IC_{50} values at pH 6 were as follows: liver, 20.9 ± 1.3 nM; brain, 18.2 ± 0.3 nM; testis, 19.2 ± 0.4 nM. *G*, dose-response relationship for CBE at pH 4.0, 5.5, and 6.0 in liver from wild-type mice in the presence or absence of detergent. Maximal activity has been set to 100%. IC_{50} values (without detergent) were as follows: pH 4.0, 3.6 ± 0.2 μM; pH 5.5 and pH 6.0, not determined. IC_{50} values (with detergent) were as follows: pH 4.0, 5.1 ± 0.3 μM; pH 5.5, 6.9 ± 0.3 μM; pH 6.0, 11.7 ± 0.7 μM. *H*, as in *G* for NB-DNJ. IC_{50} values (without detergent) were as follows: pH 4.0, not determined; pH 5.5, 17.4 ± 1.5 nM; pH 6.0, 12.0 ± 0.7 nM. IC_{50} values (with detergent) were as follows: pH 4.0, not determined; pH 5.5, 9.7 ± 0.3 μM; pH 6.0, 11.0 ± 0.7 μM.

the non-lysosomal GBA2 activity in liver. We noticed that measuring β-glucosidase activity *in vitro* in hypotonic lysates in the absence of detergent using 4-MU-β-D-glucopyranoside allows delineation of GBA1 and GBA2 activities according to their pH optimum. Under the new assay conditions, CBE completely blocked all β-glucosidase activity at pH 4.0 in hypotonic lysates from liver. The remaining activity displayed an optimum at pH 5.0–6.0 (Fig. 4*C*). *Vice versa*, NB-DNJ blocked almost all β-glucosidase activity at pH 6.0 but not at pH 4.0–4.5 (Fig. 4*C*). In the presence of both blockers, no appreciable β-glucosidase activity was measured (Fig. 4*C*). Thus, GBA2 activity can be reliably monitored, and its pH profile is distinct from that of GBA1. Therefore, GBA1 and GBA2 activities can be reliably distinguished in one and the same sample.

To confirm this result, we measured β-glucosidase activity in HEK293 cells overexpressing GBA2. NB-DNJ blocked a prominent activity around pH 6.0 (Fig. 4*D*), whereas CBE blocked β-glucosidase activity at pH 4.0 (Fig. 4*D*). Again, in the presence of both blockers, no appreciable β-glucosidase activity was measured (Fig. 4*D*). These results demonstrate that the new assay conditions allow one to distinguish between GBA1 and GBA2 activity according to their pH optimum around pH 4 and 6, respectively.

We observed three major differences when comparing our assay conditions with previous assay conditions. (*a*) In the absence of detergent, GBA1 and GBA2 activity display pH optima around pH 4 and 6, respectively. In the presence of detergent, however, the pH optimum for GBA1 activity was shifted to pH 5.5. As a consequence, between pH 5.5 and 6.5, GBA1 and GBA2 activity considerably overlap, making it difficult to distinguish between the two activities. (*b*) In the absence of detergent, GBA2 activity is 3 times higher than in the presence of detergent. (*c*) In the absence of detergent, GBA1 activity was 2 times lower than in the presence of detergent. In conclusion, the overlapping pH optima and the opposite action of detergents on GBA1 and GBA2 activities make previous assays unreliable to specifically identify the respective β-glucosidase.

To fully characterize the blockers in the absence of detergent, we determined dose-response relations for CBE and NB-DNJ using hypotonic lysates from mouse liver, brain, and testis. The IC_{50} for CBE at pH 4 was similar between tissues, ranging from 2.5 to 3.4 μM, whereas β-glucosidase activity at pH 6 was insensitive to CBE, indicating that the activity at pH 6 is independent of GBA1 (Fig. 4*E*). The IC_{50} for NB-DNJ in brain, testis, and liver at pH 6 was similar, ranging from 18.2 to 23.1 nM, whereas at pH 4, NB-DNJ did not affect β-glucosidase activity, indicating that the activity at pH 4 is independent of GBA2 (Fig. 4*F*).

To compare the actions of CBE and NB-DNJ under our new and previously used assay conditions, we determined dose-response relations for both blockers in the presence and absence of detergent. Assays were performed at pH 4 and 6, which are optimal for GBA1 and GBA2 activity in the absence of detergent, and at pH 5.5, which has been previously used to determine β-glucosidase activity in the presence of detergent (30, 33). In the absence of detergent, CBE only blocked β-glucosidase activity at pH 4.0 and not at pH 5.5 and 6.0 (Fig. 4*G*), emphasizing that under those conditions, GBA1 is only active around pH 4. In contrast, in the presence of detergent, CBE blocked β-glucosidase activity at all pH values tested (Fig. 4*G*), confirming that GBA1 activity displays a broadened and shifted pH profile in the presence of detergent. For NB-DNJ, it was not possible to determine an IC_{50} at pH 4.0 under any conditions, because GBA2 is inactive at pH 4 (Fig. 4*H*). In the absence of detergent, at pH 5.5 and 6.0, the IC_{50} was in the low nanomolar range (Fig. 4*H*). The dose-response curve was dramatically shifted to the right in the presence of detergent, resulting in IC_{50} values in the micromolar range (Fig. 4*H*). This shift could be explained either by NB-DNJ losing its potency in the presence of detergent or GBA1 or another β-glucosidase activity being sensitive to micromolar concentrations of NB-DNJ. In summary, our assay takes advantage of the different pH optimum for GBA1 and GBA2 in the absence of detergent, which allows a reliable determination of each enzyme's activity.

Tissues Differentially Express GBA1 and GBA2 Activity—We employed our assay to investigate β-glucosidase activity in hypotonic lysates from brain, testis, and liver. All three tissues displayed activities with an optimum at pH 4.0–4.5 (GBA1) and pH 5.5–6.0 (GBA2) (Fig. 5*A*). GBA2 activity was highest in the brain and lowest in the liver (Fig. 5*A*), whereas GBA1 activity was not dramatically different between tissues (Fig. 5*A*). We have shown that GBA2 is rather ubiquitously expressed in different brain areas from mice (Fig. 3*A*). In line with these results, GBA2 activity was also similar (Fig. 5*B*).

GBA2 Activity Is Down-regulated in GBA1-deficient Fibroblasts—To identify whether there is a cross-talk between GBA1 and GBA2, we compared the activities in cells from different genotypes. First, we measured the pH profile of β-glucosidase activity in brain, testis, and liver from GBA2-deficient mice. GBA2 activity at pH 6.0 was completely absent in these mice (Fig. 5*C*). The activity at pH 4.0 was sensitive to CBE, showing that this residual activity solely represents GBA1 (Fig. 5*C*). We compared GBA1 activity in wild-type and *Gba2* knockout tissue and observed no obvious difference between genotypes (Fig. 5*D*). However, because GBA1 activity is lower in the absence of detergent, we measured pH profiles in liver lysates from GBA2-deficient mice also in the presence of detergent; GBA1 activity was maximal at pH 5 and fully blocked by 30 μM CBE (Fig. 5*E*). We compared GBA1 activity between wild-type and GBA2-deficient mice in the presence of detergent at pH 5. Similar to detergent-free conditions, GBA1 activity was not dramatically different between genotypes (Fig. 5*F*).

Next, we performed the reverse experiment and measured GBA2 activity in the absence of detergent in fibroblasts from GBA1-deficient embryonic mice. GBA1 activity was absent, but also GBA2 activity was significantly reduced (Fig. 5*G*). To identify whether this is due to the lack of GBA1 protein or the lack of GBA1 activity, we measured GBA2 activity in fibroblasts from a Gaucher patient with a type II phenotype and a L444P/P415R genotype. Here, GBA1 activity was dramatically reduced, and again, GBA2 activity was also significantly decreased (Fig. 5*H*). Our results suggest that GBA2 activity depends on GBA1, but GBA1 activity is independent of GBA2.

GBA2 Activity Depends on Membrane Association—Previous studies indicated that non-lysosomal β-glucosidase activity is greatly diminished upon membrane disruption by detergents (13). However, it is not clear whether this is due to removal of

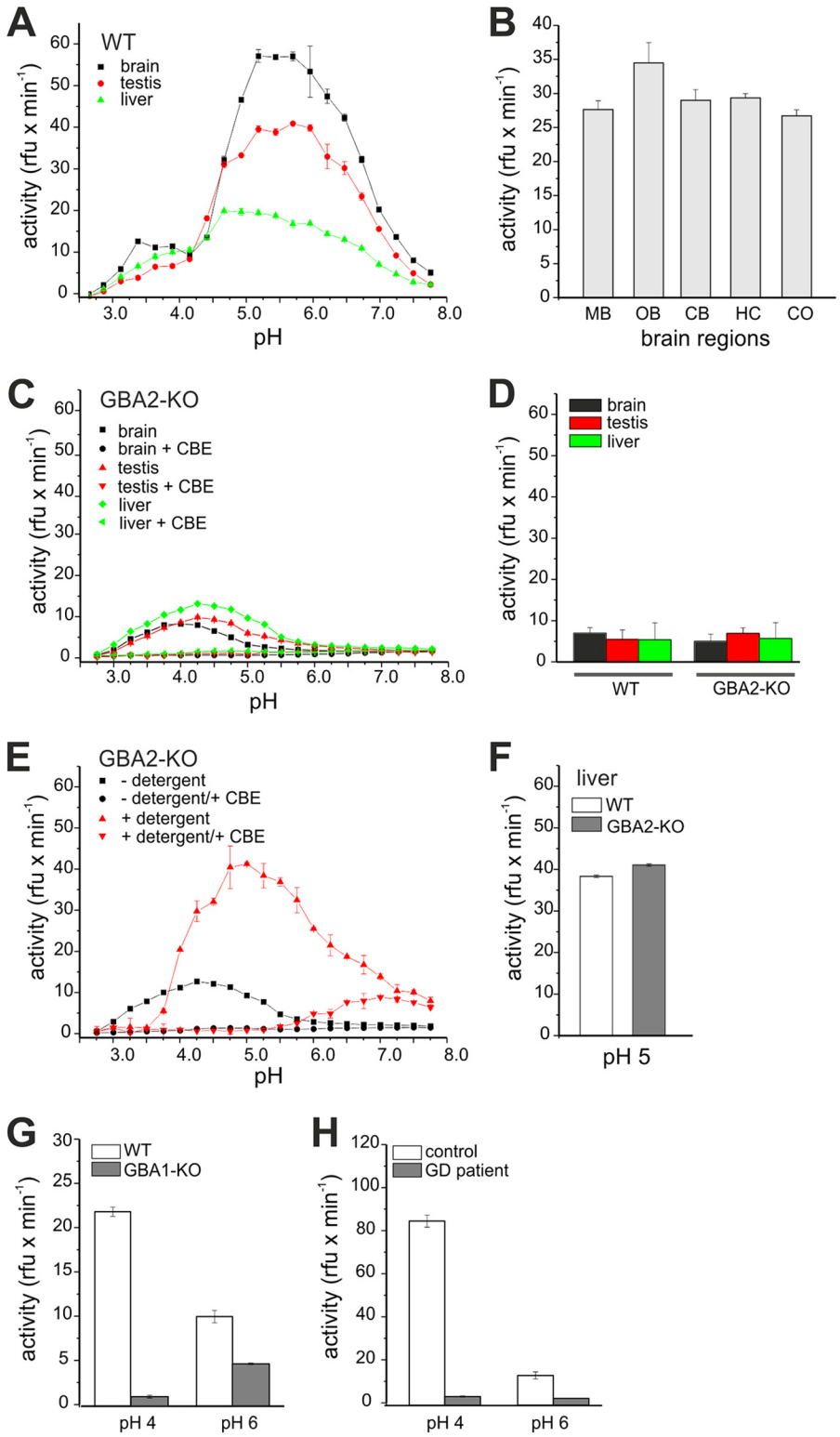

FIGURE 5. **GBA1 and GBA2 display differential activities in different tissues.** *A*, pH dependence of β-glucosidase activity in wild-type (*WT*) brain, testis, and liver. Activity was measured in hypotonic lysates in the absence of detergent using a 1.67 mM concentration of the artificial substrate 4-MU-β-D-glucopyranoside. *B*, β-glucosidase activity in different brain regions from wild-type mice (*MB*, midbrain; *OB*, olfactory bulb; *CB*, cerebellum; *HC*, hippocampus; *CO*, cortex). Activity was measured in hypotonic lysates in the absence of detergent. *C*, pH dependence of β-glucosidase activity in tissues from *Gba2* knock-out mice (*GBA2-KO*). Activity was measured as in *A* in the absence or presence of 30 μM CBE. *D*, β-glucosidase activity at pH 4 in brain, testis, and liver from wild-type (*WT*) and *Gba2* knock-out (*KO*) mice ($n = 3$). *E*, as in *C* for liver in the absence or presence of detergent. *F*, β-glucosidase activity at pH 5 in the presence of detergent in lysates from wild-type and *Gba2* knock-out liver (*GBA2-KO*). *G*, β-glucosidase activity at pH 4 and 6 in embryonic fibroblasts from wild-type and *Gba1* knock-out mice (*GBA1-KO*). *H*, β-glucosidase activity at pH 4 and 6 in human fibroblasts from a control and a Gaucher disease patient (*GD*). All data are presented as mean ± S.D. (*error bars*) Shown are representative data from one animal or one patient if not otherwise stated.

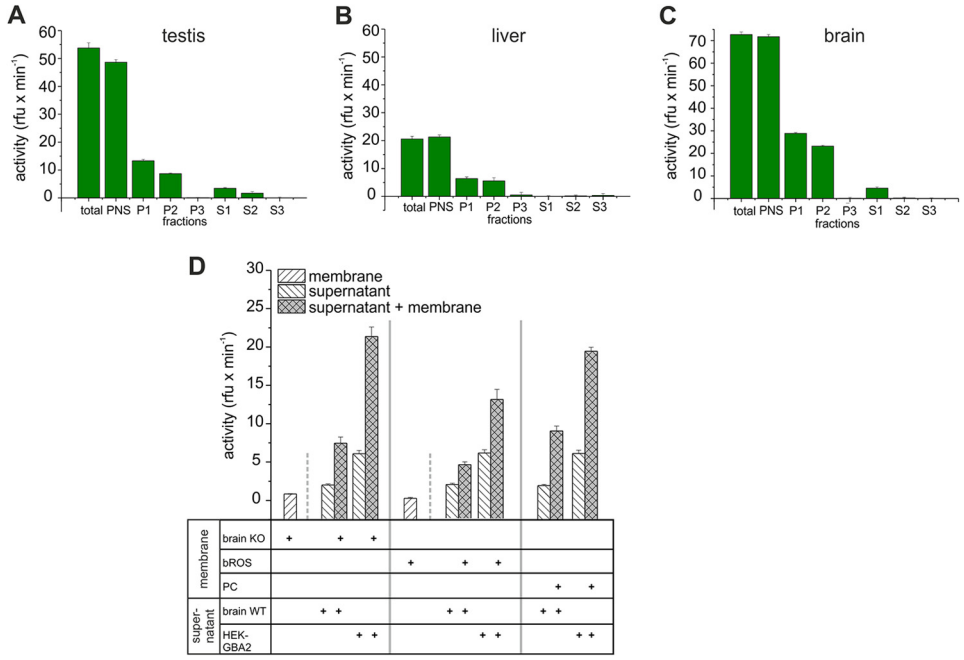

FIGURE 6. **GBA2 activity is dependent on membrane association and requires the presence of lipids.** *A*, β-glucosidase activity at pH 6 was measured using a 1.67 mM concentration of the artificial substrate 4-MU-β-D-glucopyranoside. Hypotonic lysates (*total*) from wild-type testis were centrifuged at low speed (PNS), and the pellet was subjected to multiple hypotonic washing and centrifugation steps (*1–3*). The resulting membrane (*P*) and soluble fractions (*S*) were numbered accordingly. *B*, as in *A* for liver. *C*, as in *A* for brain. Shown is a representative experiment for tissues from one wild-type mouse. *D*, β-glucosidase activity at pH 6 was measured as follows: in membrane fractions (*membrane*) from brain of *Gba2* knock-out mice (*brain KO*) and bovine rod outer segments (*bROS*), in protein-free (*PC*) liposomes, in the supernatant from brain of wild-type mice and HEK293 cells overexpressing GBA2, and in a combination of the fractions (*supernatant* + *membrane*). All data are presented as mean ± S.D. (*error bars*).

GBA2 from the membrane or a change of its enzymatic properties in the presence of detergent. Our new assay under detergent-free conditions allows the removal of GBA2 from the membrane and measurement of its activity in the presence or absence of membranes. To analyze whether GBA2 activity requires association of the enzyme with the membrane, we determined GBA2 activity in the pellet and supernatant after hypotonic washes (Fig. 6, *A*–*C*). The activity in the total fraction after hypotonic lysis and in the low speed supernatant (PNS) was similar (Fig. 6, *A*–*C*), suggesting that GBA2 activity was fully recovered in the PNS. After high speed centrifugation of the PNS, the sum of GBA2 activity in the pellet (P1) and supernatant (S1) was considerably lower than the total activity in the PNS (Fig. 6, *A*–*C*). In samples from testis and liver, GBA2 protein was almost entirely recovered in the pellet fraction (Fig. 1*F*), and in brain samples, GBA2 was about evenly distributed between the pellet and supernatant (Fig. 1*F*). In contrast, the activity in the supernatant was at least 4-fold lower compared with that in the pellet (Fig. 6, *A*–*C*). Thus, the specific GBA2 activity in the supernatant was considerably lower than what was expected from the abundance of the GBA2 protein. These results suggest that full GBA2 activity requires either a co-factor that is removed upon washing or membrane association or both.

We distinguished between these possibilities by performing several experiments. First, we determined GBA2 activity in supernatants from different hypotonic lysates in the absence or presence of membranes from *Gba2* knock-out brain. In the supernatant from wild-type brain, GBA2 activity was low (Fig. 6*D*). The addition of membranes from *Gba2* knock-out brain enhanced the activity 4-fold (Fig. 6*D*). Similarly, in the supernatant from HEK293 cells overexpressing GBA2, the activity was enhanced 4-fold by membranes from *Gba2* knock-out brain (Fig. 6*D*). Second, we determined GBA2 activity in the supernatants in the presence of membranes from bovine rod outer segment, which contain predominantly the molecules of the phototransduction cascade but lack other cell organelles and the nucleus. GBA2 activity in supernatants from both wild-type brain and HEK293 cells overexpressing GBA2 was significantly enhanced by membranes from rod outer segment (Fig. 6*D*). Third, to test whether phospholipids rather than a specific protein is responsible for the increase of GBA2 activity, we determined GBA2 activity in the presence of pure PC liposomes (Fig. 6*D*). GBA2 activity was enhanced 3– 4-fold in the presence of PC liposomes. Furthermore, the activity was similar to that in the presence of membranes from wild-type brain, demonstrating that phospholipids themselves are sufficient to restore GBA2 activity to levels observed in the presence of native membranes.

DISCUSSION

Here, we provide several new insights into the function, activity, and localization of the non-lysosomal GBA2.

First, GBA2 is not an integral membrane protein. However, it is tightly associated with membranes. One transmembrane segment was predicted from the protein sequence (20). It has been reported that GBA2 is an integral membrane protein with the C terminus in the cytosol and the N terminus either outside the cell or in the lumen of a cell organelle (19). Here, we demonstrate that the N and C termini are directly accessible from the

cytosol, ruling out any lumenal or extracellular localization. Consequently, the catalytic domain of GBA2 is also located on the cytosolic side of membranes.

Second, GBA2 is localized at the cytosolic surface of the ER and Golgi. The localization of GBA2 at the Golgi, predominantly the *cis*-Golgi, implies that GBA2 activity is in close proximity to the site of GlcCer synthesis. Furthermore, sphingomyelin synthases, which convert ceramide derived from GlcCer to sphingomyelin (13), are located at the Golgi (SMS1) or at the plasma membrane (SMS2) (34, 35). Thus, GBA2 is in close proximity not only to the site of GlcCer synthesis but also to sites where ceramide is further processed. The localization at the ER is in line with reports suggesting that GBA2 is a resident ER protein (15, 16). One model for GlcCer transport proposes that GlcCer reaches the ER through FAPP2-dependent transport and then flips to the ER lumenal side by low specificity phospholipid flippases (8, 9). In this model, GBA2 regulates GlcCer levels at the cytosolic side of the ER and, thereby, controls the amount of GlcCer that becomes available for higher order glycosphingolipid synthesis. Taken together, its localization puts GBA2 in a key position for a lysosome-independent route of GlcCer-dependent signaling.

Third, our results indicate that GBA2 activity depends on the lipid environment of the membrane, consistent with the findings that the CBE-insensitive β-glucosidase activity is lost upon membrane solubilization (13). Clearly, GBA2 must be present at the membrane, because the substrate GlcCer is either part of membranes or bound to proteins (FAPP2 and GLTP). In our assays, we use 4-MU-β-D-glucopyranoside as an artificial substrate that, in contrast to GlcCer, is water-soluble. It would be desirable to perform future studies with a membrane-bound substrate that becomes fluorescent upon hydrolysis.

To hydrolyze GlcCer, GBA1 and GBA2 have to be recruited to the membrane. Binding to the integral membrane protein LIMP-2 in the Golgi governs targeting of GBA1 to the lysosomes (36). Interaction of GBA1 with saposin C, a small glycoprotein that acts as enzymatic activator, recruits GBA1 to the membrane, thereby enabling hydrolysis of GlcCer (37). For GBA2, however, specific interaction partners and the mechanism underlying the recruitment of GBA2 to cell membranes are not known.

Under our assay conditions, we could not detect any non-lysosomal, CBE-insensitive β-glucosidase activity at neutral pH other than GBA2 (Fig. 4, *C* and *D*). This is surprising, because GBA3 (EC 3.2.1.21, Klotho-related protein) has been identified as a non-lysosomal β-glucosidase that is ubiquitously expressed and operates in a similar pH range as GBA2 (11, 12, 14). However, under detergent-containing conditions, an additional β-glucosidase activity was observed (Fig. 4, *A* and *B*). To study the relative contribution of GBA3 activity in quantitative terms, GBA3-deficient mice are required. Unfortunately, these mice are not yet available.

Another important issue concerns a potential cross-talk between GBA1- and GBA2-dependent signaling pathways. Considering the distinct subcellular localization of each enzyme, it is difficult to envision how the non-lysosomal and lysosomal pathways for GlcCer degradation interact with each other. Impairment of GBA1 activity (*e.g.* in Gaucher patients) results in accumulation of GlcCer in lysosomes of tissue macrophages, causing liver and spleen enlargement and impairment of the central nervous system (38). Gaucher disease is clinically heterogeneous and often classified into three principal subtypes: the non-neuronopathic type I, the acute neuronopathic type II, and the subacute neuronopathic type III (18). It is not possible to predict the severity of Gaucher disease manifestation, because no clear genotype-phenotype correlation exists (39, 40). However, in a recent report, GBA2 activity was measured in Gaucher patients carrying the same mutations in the *Gba1* gene but displaying distinct clinical phenotypes (41). Interestingly, GBA2 activity was different in those patients (41). The authors suggest that measuring glucosidase activity in Gaucher disease patients may provide a valuable tool to refine the classification into distinct clinical subtypes. Our results demonstrate that GBA2 activity is decreased in both fibroblasts from a patient with Gaucher disease type II and fibroblasts from GBA1-deficient mice (Fig. 5, *G* and *H*), suggesting a cross-talk between GBA1 and GBA2 that could affect the phenotype of Gaucher disease. Taken together, our study contributes to the understanding of GBA2 function in mice and might help to unravel the role of GBA2 during pathogenesis of Gaucher disease.

Acknowledgments—We thank Daniela Müller, Isabel Lux, Heike Angele, Jessica Hierer, Jens-Henning Krause, Stefanie Sonnenburg, Jeanine Klotz, and Sybille Wolf-Kümmeth for excellent technical support, Ellen Sidransky (National Institutes of Health) for providing fibroblasts from GBA1-deficient mice, Mia Horowitz (Tel Aviv University) for providing fibroblasts from a Gaucher patient, Klaus Harzer (Tübingen University) for providing control human fibroblasts, Holger Lorenz (Zentrum für Molekulare Biologie der Universität Heidelberg) for providing the constructs for the FPP assay, and Heike Krause for help with the manuscript.

REFERENCES

1. Lahiri, S., and Futerman, A. H. (2007) The metabolism and function of sphingolipids and glycosphingolipids. *Cell. Mol. Life Sci.* **64,** 2270–2284
2. Hirabayashi, Y. (2012) A world of sphingolipids and glycolipids in the brain. Novel functions of simple lipids modified with glucose. *Proc. Jpn. Acad. Ser. B Phys. Biol. Sci.* **88,** 129–143
3. Futerman, A. H., and Pagano, R. E. (1991) Determination of the intracellular sites and topology of glucosylceramide synthesis in rat liver. *Biochem. J.* **280**, 295–302
4. Jeckel, D., Karrenbauer, A., Burger, K. N., van Meer, G., and Wieland, F. (1992) Glucosylceramide is synthesized at the cytosolic surface of various Golgi subfractions. *J. Cell Biol.* **117,** 259–267
5. Paul, P., Kamisaka, Y., Marks, D. L., and Pagano, R. E. (1996) Purification and characterization of UDP-glucose:ceramide glucosyltransferase from rat liver Golgi membranes. *J. Biol. Chem.* **271,** 2287–2293
6. Lannert, H., Bünning, C., Jeckel, D., and Wieland, F. T. (1994) Lactosylceramide is synthesized in the lumen of the Golgi apparatus. *FEBS Lett.* **342,** 91–96
7. Schnaar, R. L., Suzuki, A., and Stanley, P. (2009) Glycosphingolipids. in *Essentials of Glycobiology*, 2nd Ed., Cold Spring Harbor Laboratory, Cold Spring Harbor, NY
8. Chalat, M., Menon, I., Turan, Z., and Menon, A. K. (2012) Reconstitution of glucosylceramide flip-flop across endoplasmic reticulum. Implications for mechanism of glycosphingolipid biosynthesis. *J. Biol. Chem.* **287,** 15523–15532
9. Halter, D., Neumann, S., van Dijk, S. M., Wolthoorn, J., de Mazière, A. M.,

Vieira, O. V., Mattjus, P., Klumperman, J., van Meer, G., and Sprong, H. (2007) Pre- and post-Golgi translocation of glucosylceramide in glycosphingolipid synthesis. *J. Cell Biol.* **179,** 101–115
10. D'Angelo, G., Polishchuk, E., Di Tullio, G., Santoro, M., Di Campli, A., Godi, A., West, G., Bielawski, J., Chuang, C. C., van der Spoel, A. C., Platt, F. M., Hannun, Y. A., Polishchuk, R., Mattjus, P., and De Matteis, M. A. (2007) Glycosphingolipid synthesis requires FAPP2 transfer of glucosylceramide. *Nature* **449,** 62–67
11. de Graaf, M., van Veen, I. C., van der Meulen-Muileman, I. H., Gerritsen, W. R., Pinedo, H. M., and Haisma, H. J. (2001) Cloning and characterization of human liver cytosolic β-glycosidase. *Biochem. J.* **356,** 907–910
12. Hayashi, Y., Okino, N., Kakuta, Y., Shikanai, T., Tani, M., Narimatsu, H., and Ito, M. (2007) Klotho-related protein is a novel cytosolic neutral β-glycosylceramidase. *J. Biol. Chem.* **282,** 30889–30900
13. van Weely, S., Brandsma, M., Strijland, A., Tager, J. M., and Aerts, J. M. (1993) Demonstration of the existence of a second, non-lysosomal glucocerebrosidase that is not deficient in Gaucher disease. *Biochim. Biophys. Acta* **1181,** 55–62
14. Yahata, K., Mori, K., Arai, H., Koide, S., Ogawa, Y., Mukoyama, M., Sugawara, A., Ozaki, S., Tanaka, I., Nabeshima, Y., and Nakao, K. (2000) Molecular cloning and expression of a novel klotho-related protein. *J. Mol. Med.* **78,** 389–394
15. Yildiz, Y., Matern, H., Thompson, B., Allegood, J. C., Warren, R. L., Ramirez, D. M., Hammer, R. E., Hamra, F. K., Matern, S., and Russell, D. W. (2006) Mutation of β-glucosidase 2 causes glycolipid storage disease and impaired male fertility. *J. Clin. Invest.* **116,** 2985–2994
16. Matern, H., Heinemann, H., Legler, G., and Matern, S. (1997) Purification and characterization of a microsomal bile acid β-glucosidase from human liver. *J. Biol. Chem.* **272,** 11261–11267
17. Brady, R. O., Kanfer, J. N., and Shapiro, D. (1965) Metabolism of glucocerebrosides. II. Evidence of an Enzymatic Deficiency in Gaucher's Disease. *Biochem. Biophys. Res. Commun.* **18,** 221–225
18. Hruska, K. S., LaMarca, M. E., Scott, C. R., and Sidransky, E. (2008) Gaucher disease. Mutation and polymorphism spectrum in the glucocerebrosidase gene (GBA). *Hum. Mutat.* **29,** 567–583
19. Boot, R. G., Verhoek, M., Donker-Koopman, W., Strijland, A., van Marle, J., Overkleeft, H. S., Wennekes, T., and Aerts, J. M. (2007) Identification of the non-lysosomal glucosylceramidase as β-glucosidase 2. *J. Biol. Chem.* **282,** 1305–1312
20. Matern, H., Boermans, H., Lottspeich, F., and Matern, S. (2001) Molecular cloning and expression of human bile acid β-glucosidase. *J. Biol. Chem.* **276,** 37929–37933
21. Gonzalez-Carmona, M. A., Sandhoff, R., Tacke, F., Vogt, A., Weber, S., Canbay, A. E., Rogler, G., Sauerbruch, T., Lammert, F., and Yildiz, Y. (2012) β-Glucosidase 2 knockout mice with increased glucosylceramide show impaired liver regeneration. *Liver. Int.* **32,** 1354–1362
22. Tybulewicz, V. L., Tremblay, M. L., LaMarca, M. E., Willemsen, R., Stubblefield, B. K., Winfield, S., Zablocka, B., Sidransky, E., Martin, B. M., and Huang, S. P. (1992) Animal model of Gaucher's disease from targeted disruption of the mouse glucocerebrosidase gene. *Nature* **357,** 407–410
23. Lorenz, H., Hailey, D. W., and Lippincott-Schwartz, J. (2006) Fluorescence protease protection of GFP chimeras to reveal protein topology and subcellular localization. *Nat. Methods* **3,** 205–210
24. Körschen, H. G., Beyermann, M., Müller, F., Heck, M., Vantler, M., Koch, K. W., Kellner, R., Wolfrum, U., Bode, C., Hofmann, K. P., and Kaupp, U. B. (1999) Interaction of glutamic-acid-rich proteins with the cGMP signalling pathway in rod photoreceptors. *Nature* **400,** 761–766
25. Cook, N. J., Zeilinger, C., Koch, K. W., and Kaupp, U. B. (1986) Solubilization and functional reconstitution of the cGMP-dependent cation channel from bovine rod outer segments. *J. Biol. Chem.* **261,** 17033–17039
26. Ben-Yoseph, Y., and Nadler, H. L. (1978) Pitfalls in the use of artificial substrates for the diagnosis of Gaucher's disease. *J. Clin. Pathol.* **31,** 1091–1093
27. Robinson, D. (1956) The fluorimetric determination of β-glucosidase. Its occurrence in the tissues of animals, including insects. *Biochem. J.* **63,** 39–44
28. Fujiki, Y., Hubbard, A. L., Fowler, S., and Lazarow, P. B. (1982) Isolation of intracellular membranes by means of sodium carbonate treatment. Application to endoplasmic reticulum. *J. Cell Biol.* **93,** 97–102
29. Ho, M. W., and O'Brien, J. S. (1971) Gaucher's disease. Deficiency of "acid"-glucosidase and reconstitution of enzyme activity *in vitro*. *Proc. Natl. Acad. Sci. U.S.A.* **68,** 2810–2813
30. Turner, B. M., Beratis, N. G., and Hirschhorn, K. (1977) Cell-specific differences in membrane β-glucosidase from normal and Gaucher cells. *Biochim. Biophys. Acta* **480,** 442–449
31. Legler, G. (1977) Glucosidases. *Methods Enzymol.* **46,** 368–381
32. Overkleeft, H. S., Renkema, G. H., Neele, J., Vianello, P., Hung, I. O., Strijland, A., van der Burg, A. M., Koomen, G. J., Pandit, U. K., and Aerts, J. M. (1998) Generation of specific deoxynojirimycin-type inhibitors of the non-lysosomal glucosylceramidase. *J. Biol. Chem.* **273,** 26522–26527
33. Turner, B. M., and Hirschhorn, K. (1978) Properties of β-glucosidase in cultured skin fibroblasts from controls and patients with Gaucher disease. *Am. J. Hum. Genet.* **30,** 346–358
34. Huitema, K., van den Dikkenberg, J., Brouwers, J. F., and Holthuis, J. C. (2004) Identification of a family of animal sphingomyelin synthases. *EMBO J.* **23,** 33–44
35. Yeang, C., Varshney, S., Wang, R., Zhang, Y., Ye, D., and Jiang, X. C. (2008) The domain responsible for sphingomyelin synthase (SMS) activity. *Biochim. Biophys. Acta* **1781,** 610–617
36. Reczek, D., Schwake, M., Schröder, J., Hughes, H., Blanz, J., Jin, X., Brondyk, W., Van Patten, S., Edmunds, T., and Saftig, P. (2007) LIMP-2 is a receptor for lysosomal mannose-6-phosphate-independent targeting of beta-glucocerebrosidase. *Cell* **131,** 770–783
37. Vaccaro, A. M., Tatti, M., Ciaffoni, F., Salvioli, R., Serafino, A., and Barca, A. (1994) Saposin C induces pH-dependent destabilization and fusion of phosphatidylserine-containing vesicles. *FEBS Lett.* **349,** 181–186
38. Neufeld, E. F. (1991) Lysosomal storage diseases. *Annu. Rev. Biochem.* **60,** 257–280
39. Germain, D. P., Puech, J. P., Caillaud, C., Kahn, A., and Poenaru, L. (1998) Exhaustive screening of the acid β-glucosidase gene, by fluorescence-assisted mismatch analysis using universal primers. Mutation profile and genotype/phenotype correlations in Gaucher disease. *Am. J. Hum. Genet.* **63,** 415–427
40. Lachmann, R. H., Grant, I. R., Halsall, D., and Cox, T. M. (2004) Twin pairs showing discordance of phenotype in adult Gaucher's disease. *QJM* **97,** 199–204
41. Aureli, M., Bassi, R., Loberto, N., Regis, S., Prinetti, A., Chigorno, V., Aerts, J. M., Boot, R. G., Filocamo, M., and Sonnino, S. (2012) Cell surface associated glycohydrolases in normal and Gaucher disease fibroblasts. *J. Inherit. Metab. Dis.* **35,** 1081–1091